

Hydrodynamics and Rheology of Active Liquid Crystals: A Numerical Investigation

D. Marenduzzo,¹ E. Orlandini,² and J. M. Yeomans³

¹*SUPA, School of Physics, University of Edinburgh, Mayfield Road, Edinburgh EH9 3JZ, United Kingdom*

²*Dipartimento di Fisica and Sezione INFN, Università di Padova, Via Marzolo 8, 35131 Padova, Italy*

³*The Rudolf Peierls Centre for Theoretical Physics, 1 Keble Road, Oxford OX1 3NP, United Kingdom*

(Received 9 August 2006; published 16 March 2007)

We report numerical studies of the hydrodynamics and rheology of an active liquid crystal. We confirm the existence of a transition between a passive and an active phase, with spontaneous flow in steady state. We explore how the velocity profile changes with activity, and we point out the difference in behavior for flow-aligning and tumbling materials. We find that an active material can thicken or thin under a flow, or even exhibit both behaviors as the forcing changes.

DOI: [10.1103/PhysRevLett.98.118102](https://doi.org/10.1103/PhysRevLett.98.118102)

PACS numbers: 87.10.+e, 47.50.-d, 83.60.Fg

Active viscoelastic gels and active liquid crystals are new kinds of soft matter. The gels are active in that they continuously burn energy, e.g., in the form of adenosine-triphosphate, and this pushes them out of thermodynamic equilibrium even when there is no external driving. As a consequence they exhibit exciting and nontrivial physical and rheological properties. Perhaps the most striking is that spontaneous flow can exist in nondriven active materials [1–5], in sharp contrast to their passive counterparts.

Active materials are typically encountered in biological contexts: examples are bacterial swimmers [1,2], mitotic cell extracts [6], and cytoskeletal gels with molecular motors, such as actomyosin solutions or microtubular networks with dyneins [7,8]. The activity leads to striking phenomena such as bacterial swarming and cytoplasmic streaming [1]. Furthermore, many biological gels, such as actin networks, thicken when sheared [9]. This is the opposite of the typical behavior of polymeric fluids, which flow more easily as pressure increases.

As it is often impractical to solve the equations of motion governing the microscopic dynamics of active materials, a series of coarse grained continuum models, which describe these liquid crystalline fluids in terms of a density, a velocity, and an order parameter field, have recently been proposed in the literature. References [4] consider a generalization of the Ericksen-Leslie model for liquid crystal hydrodynamics, which accounts for the activity by including extra terms that are disallowed by symmetry in the passive case. They used linear stability analysis to predict the onset of spontaneous flow and, in two dimensions, the appearance of flowing structures reminiscent of the spirals and asters seen in experiments [7]. Simha and Ramaswamy [1] have constructed and performed a stability analysis on the equations of motion for nematic and polar self-propelled particles. Liverpool and Marchetti [5] have explored a more microscopic derivation of the continuum equations for active filament solutions.

These results suggest that there is much to be learned by probing the behavior of active materials deep in the active phase or under a driving force. The continuum equations

are strongly nonlinear, and thus a robust numerical method is needed which aims to study the hydrodynamics and rheology of active fluids, not relying on any approximations other than the ones used to derive the continuum model. This is the program we aim to follow here. We use a set of equations of motion for an active liquid crystal, described by a tensorial order parameter. These are similar to those proposed in [1] and reduce to the Beris-Edwards equations of liquid crystal hydrodynamics in the passive limit. The tensorial approach allows us to describe cases in which the magnitude of local order is not constant, e.g., close to a defect core. We can also describe biaxial ordering, which may be relevant for actin networks close to the cell membrane where the distribution of tip directions is bimodal [6]. We solve the equations using a lattice Boltzmann algorithm.

Hence we can explore numerically the phase diagram of active liquid crystals confirming the presence of a transition from a passive to an active phase, characterized by spontaneous flow. We then move further into the active phase, comparing the behavior of flow-aligning and flow-tumbling materials. For flow-aligning liquid crystals, there is a highly nontrivial behavior with bands of opposing velocity forming across the cell. For the flow-tumbling case the behavior is in sharp contrast to the passive case: here we see a spatially quasiconstant director profile with a zero velocity away from the boundaries.

We also study the rheology of an active liquid crystal slab. Aligning active materials display strong shear thickening. The response of tumbling materials to an imposed flow is strikingly nontrivial: the viscosity varies nonmonotonically with increasing shear, with a pronounced maximum. We interpret this behavior as a result of the interplay between flow induced by the activity, flow induced by the forcing and the propensity of the active liquid crystal to minimize elastic distortions.

We introduce a Landau–de Gennes free energy, \mathcal{F} , to describe the equilibrium physics of the active liquid crystal in its passive phase. This is a function of a tensor order parameter, $Q_{\alpha\beta}$, whose largest eigenvalue ($2q/3$) and its

associated eigenvector, respectively, give the magnitude and direction of the local orientational order, e.g., of actin fibers in an actomyosin solution. \mathcal{F} is the integral of a sum of two free energy densities. The first is a bulk contribution,

$$\frac{A_0}{2} \left(1 - \frac{\gamma}{3}\right) Q_{\alpha\beta}^2 - \frac{A_0\gamma}{3} Q_{\alpha\beta} Q_{\beta\gamma} Q_{\gamma\alpha} + \frac{A_0\gamma}{4} \left(Q_{\alpha\beta}^2\right)^2. \quad (1)$$

A_0 is a constant and γ controls the magnitude of the ordering. (Greek indices denote Cartesian components and summation over repeated indices is implied.) A second term $K/2(\partial_\gamma Q_{\alpha\beta})^2$ describes the free energy cost of distortions in \mathbf{Q} [10], where K is an elastic constant. We neglect the spontaneous splay coefficient, equivalent to having infinitely strong anchoring at the boundaries [4].

The equation of motion for \mathbf{Q} is [11]

$$(\partial_t + \vec{u} \cdot \nabla) \mathbf{Q} - \mathbf{S}(\mathbf{W}, \mathbf{Q}) = \Gamma \mathbf{H} + \lambda \mathbf{Q}. \quad (2)$$

The first term of Eq. (2) is the material derivative describing a quantity advected by a fluid with velocity \vec{u} . This is generalized for rodlike molecules by

$$\mathbf{S}(\mathbf{W}, \mathbf{Q}) = (\xi \mathbf{D} + \mathbf{\Omega})(\mathbf{Q} + \mathbf{I}/3) + (\mathbf{Q} + \mathbf{I}/3)(\xi \mathbf{D} - \mathbf{\Omega}) - 2\xi(\mathbf{Q} + \mathbf{I}/3)\text{Tr}(\mathbf{Q}\mathbf{W}), \quad (3)$$

where Tr stands for trace, while \mathbf{D} and $\mathbf{\Omega}$ are the symmetric and the antisymmetric part, respectively, of the velocity gradient tensor $W_{\alpha\beta} = \partial_\beta u_\alpha$ [11,12]. ξ depends on the molecular details of the liquid crystal. $\mathbf{S}(\mathbf{W}, \mathbf{Q})$ appears as the order parameter distribution can be both rotated and stretched by flow gradients [11,12]. Most relevant in our context increasing ξ moves the liquid crystal from the tumbling to the aligning regime. For $\gamma = 3$, a (passive) liquid crystal is flow tumbling for $\xi \leq 0.6$ and flow aligning otherwise. In the first term on the right-hand side of Eq. (2) the molecular field \mathbf{H} is $\mathbf{H} = -\frac{\delta \mathcal{F}}{\delta \mathbf{Q}} + (\mathbf{I}/3)\text{Tr} \frac{\delta \mathcal{F}}{\delta \mathbf{Q}}$ and Γ is a collective rotational diffusion constant. The final term contains the active parameter λ . Its form was suggested on the basis of symmetry in [1] and confirmed via a microscopic derivation in [5]. For dilute or semidilute bacterial suspensions, λ should be negative, and λ^{-1} should give the time scale of relaxation of activity-induced ordering. As suggested in [4], instead, $\lambda > 0$ when describing systems which display self-alignment effects, like concentrated actomyosin solutions. However, our simulations show that for λ in the range covered in Fig. 1 (for which the order parameter q is between 0 and 1) the qualitative hydrodynamic and rheological behavior in the active phase is unchanged. These are more crucially controlled by ζ (see below).

The fluid velocity, \vec{u} , obeys the continuity equation and the Navier-Stokes equation,

$$\rho(\partial_t + u_\beta \partial_\beta) u_\alpha = \partial_\beta (\Pi_{\alpha\beta}) + \eta \partial_\beta (\partial_\alpha u_\beta + \partial_\beta u_\alpha) + (1 - 3\partial_\rho P_0) \partial_\gamma u_\gamma \delta_{\alpha\beta}. \quad (4)$$

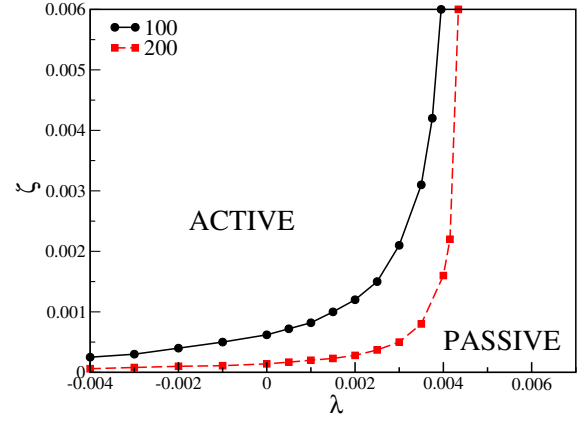


FIG. 1 (color online). Boundary between passive and active phases in the (λ, ζ) plane for an active liquid crystal, for two different system sizes. Parameters are $\xi = 0.7$, $\gamma = 3$, $\eta = 0.47$.

ρ is the fluid density, η is an isotropic viscosity and the stress tensor $\Pi_{\alpha\beta} = \Pi_{\alpha\beta}^{\text{passive}} + \Pi_{\alpha\beta}^{\text{active}}$. $\Pi_{\alpha\beta}^{\text{passive}}$ is

$$\begin{aligned} \Pi_{\alpha\beta}^{\text{passive}} = & -P_0 \delta_{\alpha\beta} + 2\xi \left(Q_{\alpha\beta} + \frac{1}{3} \delta_{\alpha\beta} \right) Q_{\gamma\epsilon} H_{\gamma\epsilon} \\ & - \xi H_{\alpha\gamma} \left(Q_{\gamma\beta} + \frac{1}{3} \delta_{\gamma\beta} \right) - \xi \left(Q_{\alpha\gamma} + \frac{1}{3} \delta_{\alpha\gamma} \right) H_{\gamma\beta} \\ & - \partial_\alpha Q_{\gamma\nu} \frac{\delta \mathcal{F}}{\delta \partial_\beta Q_{\gamma\nu}} + Q_{\alpha\gamma} H_{\gamma\beta} - H_{\alpha\gamma} Q_{\gamma\beta}. \end{aligned} \quad (5)$$

P_0 is a constant. The active stress is given to linear order by $\Pi_{\alpha\beta}^{\text{active}} = -\zeta Q_{\alpha\beta}$ [1]. This term determines the hydrodynamics in the active phase. $\zeta > 0$ and $\zeta < 0$ refer, respectively, to extensile and contractile active gels [1,3–5]. Although systematic investigations of the values of ζ are still lacking, experiments [8] and microscopic approaches [5], suggest that actomyosin gels are contractile.

These equations of motion reduce to the Beris-Edwards description of liquid crystal hydrodynamics for $\lambda = \zeta = 0$. In the limit of a uniaxial order parameter of constant magnitude they map to the equations derived in [3,4] to describe an active gel in terms of the polarization field.

We solve Eqs. (2) and (4) by using a lattice Boltzmann approach. This is a generalization of the algorithm described in Refs. [12], which was devised to study the hydrodynamics and rheology of a passive liquid crystal. The active contributions needed here simply modify the forcing terms in the lattice Boltzmann algorithm.

We first investigate the flow fields set up by the activity, comparing flow-aligning and flow-tumbling materials. Consider a slab of active liquid crystal sandwiched between two fixed plates, parallel to the xz plane, lying a distance L apart along the y axis and with homogeneous anchoring (along \hat{x}) at the boundaries $y = 0, L$.

In what follows we will mainly use simulation units. These can be related to physical units by noting that one space and time simulation unit correspond to $\Delta x = 0.025 \mu\text{m}$ and $\Delta t = 0.067 \mu\text{s}$, respectively, if we choose

a rotational viscosity γ_1 [10] and an elastic constant K of 1 Poise and 25 pN, respectively.

Figure 1 shows the behavior in the (λ, ζ) plane for two different system sizes $L = 100$ and $L = 200$. We confirm the presence of a transition between a passive and an active phase, predicted analytically in Refs. [3,4,13]. In the passive phase, which occurs for small L or for small ζ , there is no flow and the polarization field is homogeneous. In the active state, however, there is a spontaneous flow along x which is initially approximately sinusoidal with a half wavelength between the channel walls.

Staying at $\lambda = 0.002$ and $L = 400$ we increase ζ so as to move the system further into the active phase. Results, for the velocity and the corresponding angle the liquid crystal director makes with the x axis, θ are shown in Figs. 2(a) and 2(b), respectively, for the flow-aligning case. The velocity is initiated with a small random component. The first striking feature is that the number of wavelengths in the velocity profile increases with ζ . For $L = 400$ and a zero velocity starting configuration states with 1/2, 1, and 3 wavelengths across the channel are formed as ζ is increased, a behavior reminiscent of shear banding in nonactive materials [14]. The magnitude of the velocity is $\sim L^2$ and states with a larger number of wavelengths appear at a higher ζ for smaller L . There are strong hysteresis effects with the final state depending on the initial condition. For instance, starting with a single wavelength state and increasing ζ new, weaker bands are formed, but then disappear.

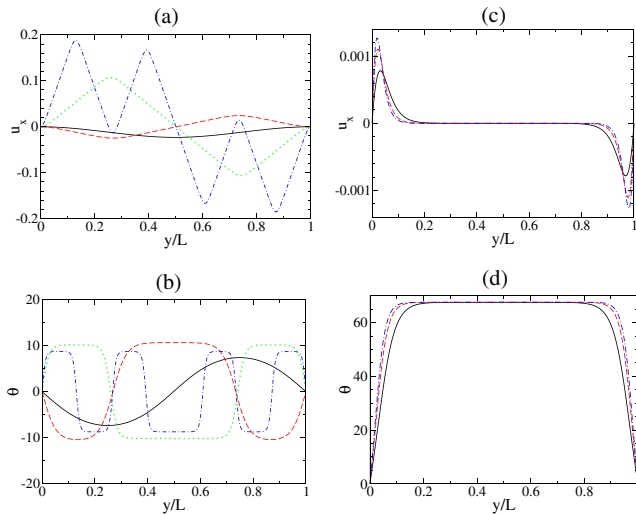


FIG. 2 (color online). Velocity (top) and director angle to the x axis (bottom) profiles for (a),(b) an active aligning liquid crystal ($\xi = 0.7$, $\gamma = 3$, $\lambda = 0.002$, $L = 400$) and (c),(d) an active tumbling ($\xi = 0.6$, $\gamma = 3$, $\lambda = 0.002$, $L = 400$) liquid crystal for different values of ζ . In (a),(b) solid, long-dashed, dotted, and dot-dashed line correspond to $\zeta = 0.0001$, 0.0012, 0.005, and 0.02, respectively. In (c),(d) solid, long-dashed, and dot-dashed lines correspond to $\zeta = -0.0003$, -0.0006 , and -0.0008 , respectively. In (b) the solid line has been multiplied by 10 to fit the scale. (All numbers are in simulation units.)

As ζ increases the sinusoidal variation of the velocity is replaced by areas of constant shear separated by narrow regions where the shear gradient reverses. This is because backflow acts to minimize elastic distortions and hence favors constant shear corresponding to the plateaus in the director angle, shown in Fig. 2(b). Here the inclination angle of the director is close to the usual Leslie value [10].

In a nonactive liquid crystal, as ξ is decreased, there is no real solution for the shear-induced angle and the director tumbles in the flow. However flow-tumbling materials yield a markedly different phenomenology in the active phase. The velocity is zero and the director field takes a constant value independent of position except near the channel walls as shown in Figs. 2(c) and 2(d). (An investigation of the Leslie-Ericksen-Parodi equations of motion shows that there is indeed a new solution which is only present for nonzero activity.)

We now analyze the rheological response of an active liquid crystal to a Poiseuille flow driven by a pressure difference Δp along x . Figure 3 shows the velocity profiles for two different values of Δp , while Fig. 4 maps out the viscosity (scaled to the Newtonian value) as a function of the dimensionless ratio $\Delta p L^2 / (\eta v_0)$, where $v_0 \equiv \Delta x / \Delta t$. Results are shown for $\zeta = 0.005$ and 0.05, which correspond to velocity modulations of 1/2 and 3/2 wavelengths, respectively. In the former case, for very small forcing, the maximum velocity attained by the aligning active liquid crystal is about 1 order of magnitude larger than that of its passive counterpart. This is because the spontaneous flow adds to the externally imposed flow. As the forcing is increased, the activity-induced ordering, which leads to spontaneous flow, is gradually replaced by a Δp -induced ordering, which does not, and as a result the fluid shear thickens to its passive viscosity (Fig. 4).

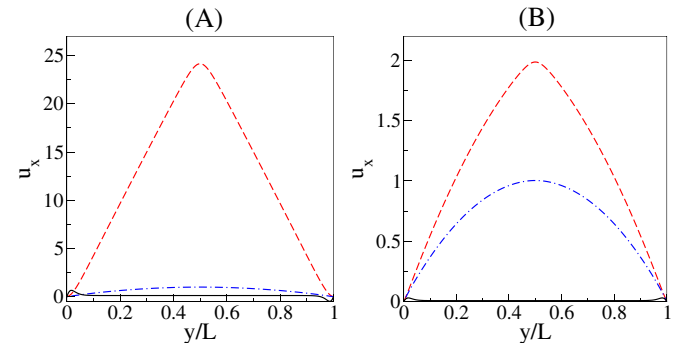


FIG. 3 (color online). Velocity profiles for active aligning (long-dashed line), active tumbling (solid line), and passive (dot-dashed line) liquid crystals under two different forcings. A and B are indicated in Fig. 4. Parameters are: $\lambda = 0.001$, $\gamma = 3$, $L = 200$, while ξ and ζ were 0.6 and -0.005 for flow tumbling, 0.7 and 0.005 for flow aligning, and 0.7 and 0 for passive liquid crystals, respectively. In A $\Delta p L^2 / (\eta v_0)$ was 0.035 and in B it was 0.85 (see Fig. 4). The values of u_x have been rescaled by the maximum u_x attained in the passive case.

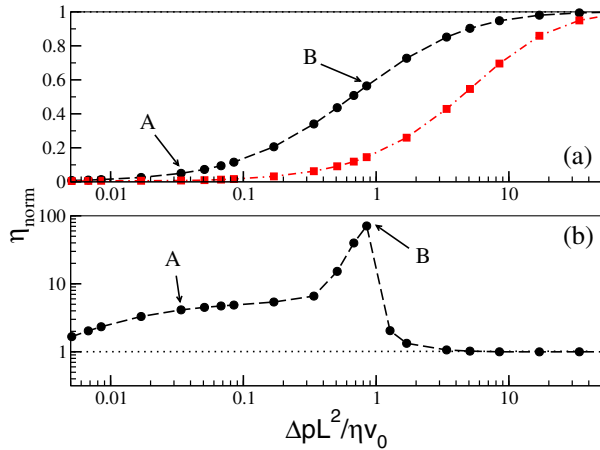


FIG. 4 (color online). Plot of the viscosity, scaled to the Newtonian value, versus dimensionless forcing for (a) aligning and (b) tumbling liquid crystals. Parameters for the dashed lines (solid circles) are as in Fig. 3 except for Δp which is changed systematically. The dot-dashed line (solid squares) is for a flow-aligning liquid crystals deeper in the active phase with $\zeta = 0.05$ (other parameters remain the same). Any deviation from 1 (dotted line) indicates a viscoelastic behavior.

Tumbling active materials display an even richer phenomenology. We consider $\zeta = -0.005$ corresponding to the velocity profile in Fig. 3. For slow forcing flow near the left-hand boundary is enhanced and that near the right-hand boundary opposed by the pressure gradient. Hence an asymmetry is introduced in the velocity profile. As forcing is increased the symmetry of the primary flow is restored. There is an enormous shear-thickening and the viscosity reaches a value ~ 100 -fold larger than that experienced by a passive liquid crystal under the same conditions. This is a phenomenon akin to permeation in cholesteric passive liquid crystals [12]: the liquid crystal is trying to maintain a director field aligned at a constant angle. When the forcing is increased further, the tumbling active material is unable to maintain this state and it undergoes abrupt shear thinning. The order introduced by the activity is destroyed, the director lines up along the applied flow, and the behavior of a passive gel is recovered as expected. We have run another set of simulations with contractile flow-aligning materials (which are passive when $\Delta p = 0$), with the same value of ζ . These also showed a nonmonotonic response, although with a smaller maximum apparent viscosity. This striking behavior is a result of the propensity of the contractile gel to minimize elastic distortions when a flow is induced by the forcing. Our calculation suggests that contractility may be another reason underlying the thickening of biological gels under shear observed in [9]. Repeating the experiments in [9] with extensible gels would allow this effect to be singled out.

In conclusion, we have investigated numerically the hydrodynamics and rheology of an active liquid crystal moving deep into the active phase. Tumbling and aligning

active materials have very different behavior. In aligning liquid crystals velocity bands are formed. Strong hysteresis suggests a very complicated phase space with many competing metastable states. Tumbling active liquid crystals select, in contrast to their passive counterparts, a state with a constant director field in the bulk of the sample which only flows close to the boundaries.

Activity leads to strong shear thickening in aligning liquid crystals, while the apparent viscosity of active tumbling materials shows a striking nonmonotonic behavior with a narrow high peak in which flow is considerably slower than in an equivalent passive gel. An analogous phenomenon occurs for contractile aligning gels.

Our predictions could be ideally tested with rheological experiments on actomyosin solutions or on microtubular networks with dynein, in which cross-linkings are active and dynamic and for which there is evidence that this continuum model captures the physics observed in the experiments [1,3]. Cell extracts are likely to be less ideal candidates for an experimental validation of our results, as rigid branching points may render their passive equivalent closer to an elastomer than to a liquid crystal.

We thank M. E. Cates for useful discussions.

-
- [1] R.A. Simha and S. Ramaswamy, Phys. Rev. Lett. **89**, 058101 (2002); Y. Hatwalne *et al.*, Phys. Rev. Lett. **92**, 118101 (2004).
 - [2] I. Llopis and I. Pagonabarraga, Europhys. Lett. **75**, 999 (2006); S. Ramachandran, P. B. S. Kumar, and I. Pagonabarraga, Eur. Phys. J. E **20**, 151 (2006).
 - [3] K. Kruse *et al.*, Eur. Phys. J. E **16**, 5 (2005); K. Kruse *et al.*, Phys. Rev. Lett. **92**, 078101 (2004).
 - [4] R. Voituriez, J. F. Joanny, and J. Prost, Europhys. Lett. **70**, 404 (2005); Phys. Rev. Lett. **96**, 028102 (2006).
 - [5] T. B. Liverpool and M. C. Marchetti Phys. Rev. Lett. **90**, 138102 (2003); Europhys. Lett. **69**, 846 (2005); Phys. Rev. Lett. **97**, 268101 (2006).
 - [6] D. Bray, *Cell Movements: From Molecules to Motility* (Garland, New York, 2000).
 - [7] T. Surrey *et al.*, Science **292**, 1167 (2001); F. J. Nedelec *et al.*, Nature (London) **389**, 305 (1997).
 - [8] O. Thoumine and A. Ott, J. Cell Sci. **110**, 2109 (1997).
 - [9] C. Storm *et al.*, Nature (London) **435**, 191 (2005).
 - [10] P. G. de Gennes and J. Prost, *The Physics of Liquid Crystals* (Clarendon, Oxford, 1993), 2nd ed.
 - [11] A. N. Beris and B. J. Edwards, *Thermodynamics of Flowing Systems* (Oxford University, Oxford, 1994).
 - [12] C. Denniston *et al.*, Phil. Trans. R. Soc. A **362**, 1745 (2004); D. Marenduzzo, E. Orlandini, and J. M. Yeomans, Phys. Rev. Lett. **92**, 188301 (2004); C. M. Care and D. J. Cleaver, Rep. Prog. Phys. **68**, 2665 (2005).
 - [13] The transition occurs at a value of ζ, ζ_c , which is $\propto L^{-2}$.
 - [14] S. M. Fielding and P. D. Olmsted, Phys. Rev. Lett. **92**, 084502 (2004).